JOURNAL OF SOLID STATE CHEMISTRY 82, 8–13 (1989)

Metal–Insulator Transition in the System $(Gd_{1-x}Ca_x)MnO_{2.98}$

H. TAGUCHI* AND M. NAGAO

Research Laboratory for Surface Science, Faculty of Science, Okayama University, Okayama 700, Japan

AND M. SHIMADA

Department of Applied Chemistry, Faculty of Engineering, Tohoku University, Sendai 980, Japan

Received February 27, 1989; in revised form April 17, 1989

The electrical resistivity of $(Gd_{1-x}Ca_x)MnO_{2.98}$ ($0.5 \leqq x \leqq 0.9$) was measured in the temperature range 80 to 900 K. At low temperature, manganates are semiconductors, and the electrical resistivity follows the Mott's $T^{-1/4}$ law, indicating the possible occurrence of variable range hopping of electrons due to Anderson localization. At high temperature, manganates ($0.6 \leqq x \leqq 0.9$) exhibit a metal–insulator transition without any crystallographic change. From the results of the magnetic susceptibility measurement, it is concluded that the metal–insulator transition is caused by a change in the spin state of trivalent manganese ion in $(Gd_{1-x}Ca_x)MnO_{2.98}$.

Introduction

$CaMnO_3$ has an orthorhombic perovskite-type structure with $a = 0.5282$ nm, $b = 0.5265$ nm, and $c = 0.7452$ nm (*1*). $CaMnO_3$ exhibits a weak ferromagnetism with $T_N = 123$ K (*2*), and is an *n* type semiconductor (*2*). At low temperature $\log \rho$ vs $T^{-1/4}$ is linear, and the electrical properties of $CaMnO_3$ are explained by the variable range hopping of electrons due to Anderson localization (*3*).

Many investigations have been reported on the substitution of Ca^{2+} ion by rare earth ions in $CaMnO_3$. Taguchi *et al.* reported the electrical properties of $(Ln_{1-x}Ca_x)MnO_3$ (*Ln*: La and Nd) (*4, 5*). These manganates exhibit *n*-type semiconducting behavior below room temperature. The electrical resistivity follows the Mott's $T^{-1/4}$ law, indicating the possible occurrence of variable range hopping of electrons due to Anderson localization. The resistivity of these manganates has a positive temperature coefficient at high temperature, and a metal–insulator transition occurs without a change in the crystallographic parameter. The metal–insulator transition temperature decreases with decreasing ionic radius of the rare-earth ion.

$GdMnO_3$ has an orthorhombic perovskite structure, and the cell constants are $a = 0.5310$ nm, $b = 0.5840$ nm, $c = 0.7430$ nm (*6*). The ionic radius of the Gd^{3+} ion with a coordination number of 12 is smaller than those of La^{3+} and Nd^{3+} ions (*7*). In the

* To whom correspondence should be addressed.

0022-4596/89 $3.00

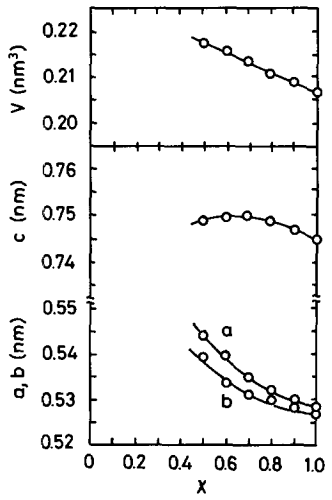

FIG. 1. Cell constants and cell volume vs composition for the system $(Gd_{1-x}Ca_x)MnO_{2.98}$.

present study, the perovskite materials $(Gd_{1-x}Ca_x)MnO_{3-\delta}$ ($0.5 \leqq x \leqq 0.9$) were synthesized in order to study the electrical transport mechanism by means of electrical resistivity and magnetic susceptibility measurements. These results provide information for the discussion of the behavior of the $3d$ electrons of Mn ions in the perovskite-type oxide system.

Experimental

All $(Gd_{1-x}Ca_x)MnO_{3-\delta}$ ($0.5 \leqq x \leqq 0.9$) samples were prepared by a standard ceramic technique. Powders of Gd_2O_3, $CaCO_3$, and $MnCO_3$ were weighed in the appropriate proportions and milled for 12 hr with acetone. After the mixed powders were dried at 373 K, they were calcined in air at 1073 K for 24 hr, and then fired at 1623 K for 24 hr under a stream of pure oxygen gas. For measuring the electrical resistivity, the powder was pressed into a pellet form under a pressure of 50 MPa, and the pellet sintered at 1623 K for 12 hr under pure oxygen. The oxygen-deficient materials obtained in this way were annealed at 973 K under pure oxygen for 24 hr.

The phases of the samples were identified by X-ray powder diffraction with Ni-filtered Cu$K\alpha$ radiation. The cell constants of the samples were determined from high-angle reflections with Si as a standard. The oxygen content in each sample was determined by the oxidation–reduction (redox) method (*5*).

The electrical resistivity was measured by a standard four-electrode technique in the temperature range 80 to 900 K. The magnetic susceptibility was measured by a magnetic torsion balance in the temperature range 80 to 750 K. The phase transition of the samples was monitored by differential thermal analysis (DTA) in the temperature range 300 to 1273 K.

Results and Discussion

The oxygen content of $(Gd_{1-x}Ca_x)MnO_{3-\delta}$ ($0.5 \leqq x \leqq 0.9$) annealed at 973 K under pure oxygen was determined to be 2.98 ($\delta = 0.02$) from the chemical analysis, and independent of the composition. X-ray powder diffraction patterns of $(Gd_{1-x}Ca_x)MnO_{2.98}$ were completely indexed as the orthorhombic perovskite-type structure. The relation between the cell constants and the composition is shown in Fig. 1. Both a-axis and b-axis decrease with increasing x, and the c-axis has a maximum value at ca. $x = 0.8$. The cell volume monotonously decreases with increasing x. The ionic radii of Ca^{2+} and Gd^{3+} ions with coordination number (CN) of 12 are 0.135 nm and 0.106 nm, respectively (*7*). Despite the fact that the ionic radius of Ca^{2+} is larger than that of Gd^{3+}, the cell volume decreases with increasing Ca^{2+} ion content. This linear decrease in the cell volume is explained by the increase of Mn^{4+} ion content; that is, the ionic radius of the Mn^{4+} ion is smaller than that of the Mn^{3+} ion located at the octahedral site (*7*).

The electrical resistivity data of $(Gd_{1-x}Ca_x)MnO_{2.98}$ in the temperature range 80 to

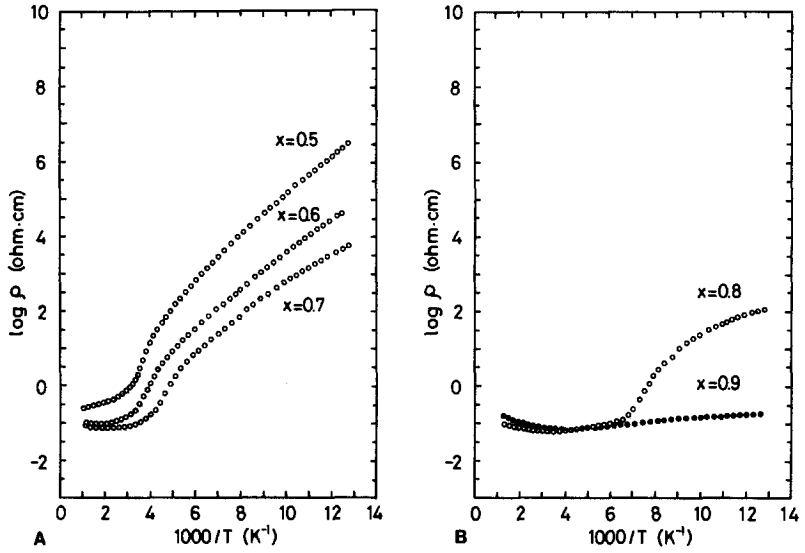

FIG. 2. Electrical resistivity vs $1/T$ for the system $(Gd_{1-x}Ca_x)MnO_{2.98}$.

1000 K is shown in Fig. 2. Below room temperature, all the manganates were semiconductors and the electrical resistivity decreased with increasing x. At low temperature, a plot of log ρ vs $1000/T$ was nonlinear analogous to the results of the electrical properties of $(Ln_{1-x}Ca_x)MnO_3$ (*Ln*: La and Nd) (*4*, *5*).

The relation of log ρ vs $T^{-1/4}$ in $(Gd_{1-x}Ca_x)MnO_{2.98}$ is shown in Fig. 3. As seen in Fig. 3, the log ρ vs $T^{-1/4}$ plot is linear in the temperature range 90–250 K, and log ρ strongly depends on the chemical composition. Joshi *et al.* reported the electrical properties of $(Eu_{1-x}Sr_x)FeO_3$ (*8*). At high temperature, log ρ vs $1000/T$ is linear, but, at low temperature, log ρ follows Mott's $T^{-1/4}$ law, indicating the possible occurrence of variable range hopping of electrons due to Anderson localization (*3*). From these results, the electrical properties of $(Gd_{1-x}Ca_x)MnO_{2.98}$ can be related to variable range hopping of electrons due to Anderson localization, which was also reported for other perovskite systems such as $(Eu_{1-x}Sr_x)FeO_3$ (*8*), $CaMnO_{3-\delta}$ (*9*), and $(Ln_{1-x}Ca_x)MnO_3$ (*Ln*: La and Nd) (*4*, *5*).

The relation between electrical resistivity and temperature in the range 200–1000 K is shown in Fig. 4. At high temperature, the resistivity had a positive temperature coefficient and the electrical resistivity linearly increased with increasing temperature in

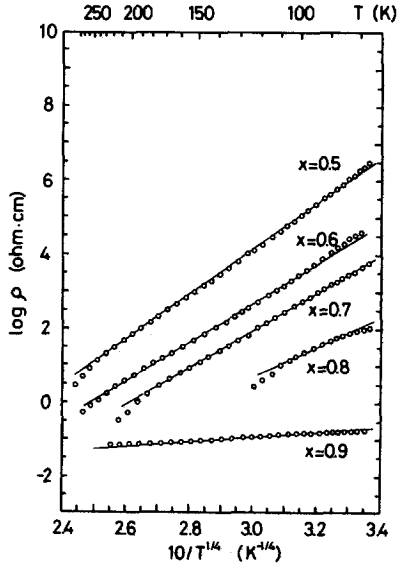

FIG. 3. Electrical resistivity vs $T^{-1/4}$ for the system $(Gd_{1-x}Ca_x)MnO_{2.98}$.

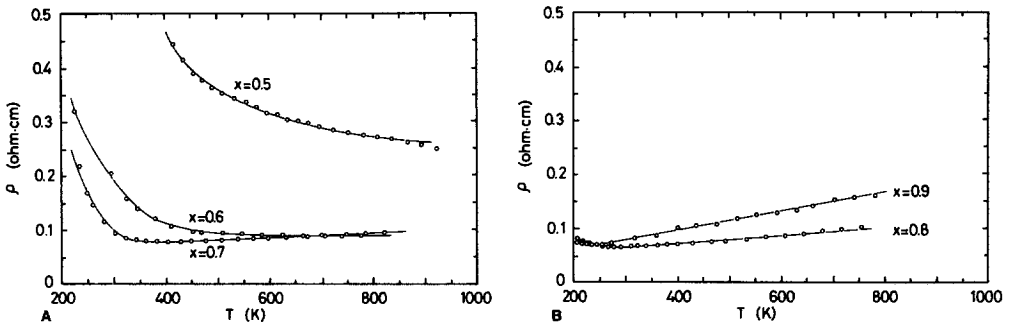

FIG. 4. Electrical resistivity vs T for the system $(Gd_{1-x}Ca_x)MnO_{2.98}$.

the range $0.6 \leqq x \leqq 0.9$. From these results, $(Gd_{1-x}Ca_x)MnO_{2.98}$ ($0.6 \leqq x \leqq 0.9$) exhibits a metal–insulator transition. We define the metal–insulator transition temperature (T_t) as the temperature where resistivity coefficient changes from negative to positive. The relation between T_t and the composition is shown in Fig. 5, together with T_t of $(Ln_{1-x}Ca_x)MnO_3$ (Ln: La and Nd) (*4, 5*). T_t decreased with increasing x. At a constant composition, T_t decreases with decreasing ionic radius of the Ln^{3+} ions. From the results of DTA measurements on $(Gd_{1-x}Ca_x)MnO_{2.98}$ ($x = 0.6$ and 0.7), no exothermic or endothermic peaks were found close to T_t. This fact indicates that the metal–insulator transition in $(Gd_{1-x}Ca_x)MnO_{2.98}$ occurs without a phase transition in analogy with $(Ln_{1-x}Ca_x)MnO_3$ (Ln: La and Nd) (*4, 5*).

From the magnetic susceptibility measurements on $(Gd_{1-x}Ca_x)MnO_{2.98}$, positive values of paramagnetic Curie temperature (T_θ) were obtained in the range $0.6 \leqq x \leqq 0.9$. The temperature dependence of the inverse susceptibility ($1/\chi$) in $(Gd_{1-x}Ca_x)MnO_{2.98}$ is shown in Fig. 6. In Fig. 6, the hatchings indicate the metal–insulator transition temperature (T_t) as shown in Fig. 5. The $1/\chi$-T curves follow the Curie–Weiss law at high temperature, and a change in slope can be seen at ca. 490 K, 440 K, 310 K, and 260 K, for $x = 0.6$, 0.7, 0.8, and 0.9, respectively; it is obvious that this change in slope coincides with the metal–insulator transition temperature (T_t), deduced from the resistivity measurements.

In the range $0.6 \leqq x \leqq 0.7$, the slopes of $1/\chi$-T curves below T_t were larger than those above T_t. On the other hand, in the range $0.8 \leqq x \leqq 0.9$, the slope of $1/\chi$-T curves below T_t deviate from Curie–Weiss law. It is believed that this deviation is caused by the residue of clusters consisting of parallel or antiparallel spins (*10*). The effective magnetic moment (μ_{eff}) calculated

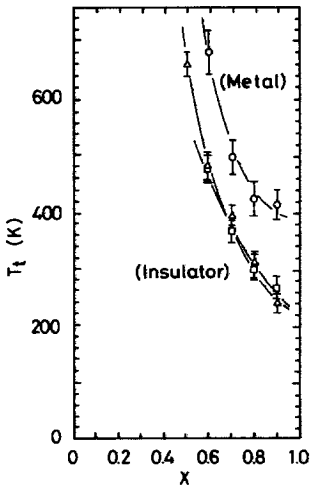

FIG. 5. Metal–insulator transition temperature vs composition for the system $(Ln_{1-x}Ca_x)MnO_{3-\delta}$. (○) La, (△) Nd, (□) Gd.

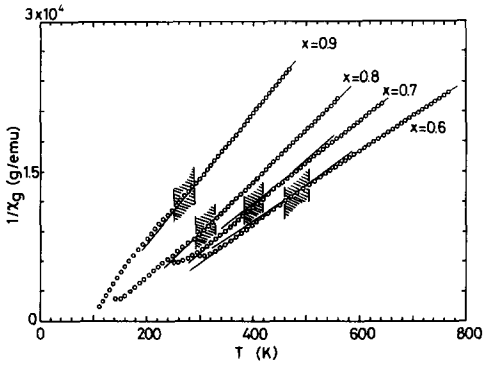

FIG. 6. Inverse magnetic susceptibility vs temperature for the system $(Gd_{1-x}Ca_x)MnO_{2.98}$.

from the linear portions below and above the deflection point in the $1/\chi$-T curves are listed in Table I. The present results suggest that a change in the electron configuration of Mn ions in $(Gd_{1-x}Ca_x)MnO_{2.98}$ affects the electrical conductivity.

The energy band scheme for the perovskite-type structure proposed by Goodenough (*11*) was adopted for the interpretation of the electrical properties in $(Ln_{1-x}Ca_x)MnO_3$ (*Ln*: La and Nd) (*4, 5*). The band scheme consists of partially filled σ^* electron and π^* hole states. The localized π^* orbitals of α and β spins at a given cation are split by the intraatomic exchange (E_{ex}); the itinerant σ^* orbitals are likewise split by E_{ex}. The magnitude of the electrostatic field (Δ) depends on both the particular anion complex and the valency state of the cation. In the present system, the values of μ_{eff} in $(Gd_{1-x}Ca_x)MnO_{2.98}$ change at the metal–insulator transition temperature, as shown in Table I. The Mn^{4+} ions ($3d^3$) have the electron configuration $(d\varepsilon)^3(d\gamma)^0$. On the other hand, for the Mn^{3+} ion ($3d^4$), two types of electron configuration can be proposed: one is the low-spin state, $(d\varepsilon)^4(d\gamma)^0$, and the other is the high-spin state $(d\varepsilon)^3(d\gamma)^1$. As seen in Table I, the observed values are in agreement with the calculated values in the range $0.6 \leqq x \leqq 0.7$. It is postulated that the low-spin state of Mn^{3+} ions exists below T_t, and that the spin state of Mn^{3+} ion changes from low to high above T_t. Since the electrons partially fill both itinerant σ^* and localized π^* orbitals, $(Gd_{1-x}Ca_x)MnO_{2.98}$ exhibits metallic behavior above T_t.

TABLE I

THE EFFECTIVE MAGNETIC MOMENT (μ_{eff}) IN THE SYSTEM $(Gd_{1-x}Ca_x)MnO_{2.98}$

	μ_{eff} (Observed)		μ_{eff} (Calculated)[a]	
X	Insulator region	Metal region	Insulator region	Metal region
0.6	6.26	6.58	6.07	6.62
0.7	5.53	5.81	5.60	6.06
0.8	—	5.04	5.08	5.44
0.9	—	4.40	4.50	4.74

[a] Gd^{3+}: $\mu_{eff} = 7.9\ \mu_B$ (*12*).

The Weiss constant (T_θ) of $x = 0.6$ and 0.7 above T_t is lower than that below T_t. It is considered that the correlation between the small polarons below T_t will tend to keep Mn^{4+} ions as near neighbors of Mn^{3+} ions such as $(La_{1-x}Ca_x)MnO_3$ (*13*), which favors a ferromagnetic superexchange via Mn^{3+}–O–Mn^{4+} interaction. Above T_t, the polaron ordering is suppressed, and the net ferromagnetic exchange interaction may be decreased. Consequently, T_θ above T_t is lowered.

In order to discuss the influence of the Mn–O–Mn interaction, it will be necessary to measure the Hall coefficient and the thermoelectric power of this system in the near future. This will provide useful information for explaining the mechanism of metal–insulator transition for this system.

It is concluded that $(Gd_{1-x}Ca_x)MnO_{2.98}$ ($0.6 \leqq x \leqq 0.9$) exhibits the metal–insulator transition without a phase transition at high temperature analogous to $(Ln_{1-x}Ca_x)MnO_3$ (*Ln*: La and Nd). The value of μ_{eff} changes in the neighborhood of the metal–insulator transition temperature (T_t), and the electri-

cal properties are influenced by the electron configuration of the Mn ion.

References

1. H. TAGUCHI, M. NAGAO, T. SATO, AND M. SHIMADA, *J. Solid State Chem.* **78,** 312 (1989).
2. J. B. MACCHESNEY, H. WILLIAM, J. F. POTTER, AND R. C. SHERWOOD, *Phys. Rev.* **164,** 779 (1967).
3. N. F. MOTT, *Adv. Phys.* **21,** 785 (1972).
4. H. TAGUCHI AND M. SHIMADA, *J. Solid State Chem.* **62,** 290 (1986).
5. H. TAGUCHI, M. NAGAO, AND M. SHIMADA, *J. Solid State Chem.* **76,** 284 (1988).
6. G. J. MCCARTHY, P. V. GALLAGHER, AND C. SIPE, *Mater. Res. Bull.* **8,** 1277 (1973).
7. R. D. SHANNON AND C. T. PREWITT, *Acta Crystallogr. B* **25,** 925 (1969).
8. V. JOSHI, O. PARKASH, G. N. RAO, AND C. N. R. RAO, *J. Chem. Soc. Faraday Trans.* **2,** 75 (1979).
9. H. TAGUCHI, *Phys. Status Solidi A* **88,** K79 (1985).
10. S. CHIKAZUMI, "Physics of Ferromagnetism," Vol. 1, p. 136, Syokabo, Tokyo (1978). [in Japanese]
11. J. B. GOODENOUGH, *J. Appl. Phys.* **37,** 1415 (1966).
12. T. SHIN-IKE, T. SAKAI, G. ADACHI, AND J. SHIOKAWA, *Mater. Res. Bull.* **12,** 831 (1977).
13. J. B. GOODENOUGH, "Magnetism and the Chemical Bond," p. 229, Wiley, New York (1963).